The phonon spectrum injected by a metallic point contact : an FLN study

1990 J. Phys.: Condens. Matter 2 6721

(http://iopscience.iop.org/0953-8984/2/32/002)

J. Phys.: Condens. Matter 2 (1990) 6721–6729. Printed in the UK

The phonon spectrum injected by a metallic point contact: an FLN study

M J van Dort, K Z Troost, J I Dijkhuis and H W de Wijn
Faculty of Physics and Astronomy, University of Utrecht, PO Box 80.000, 3508 TA Utrecht, The Netherlands

Received 19 February 1990, in final form 26 April 1990

Abstract. A metallic point contact, consisting of a tungsten whisker pressed onto a tungsten film, is used to inject high-frequency phonons into a ruby crystal kept at 1.5 K. The effective phonon temperature near the point contact is measured via the temperature dependences of the position and width of the R_1 line of the Cr^{3+}. High spectral resolution is provided by the technique of fluorescence line narrowing. The temperatures observed range up to 300 K, demonstrating the effectiveness of the point contact as a generator of high-frequency phonons.

1. Introduction

In the 1960's the study of high-frequency acoustic phonons in solids received a new impulse when von Gutfeld and Nethercot [1] introduced Joule heaters as pulsed phonon generators. Non-equilibrium phonons were injected by heating a metal film deposited on the crystal, which was kept at liquid-He temperatures to freeze out thermal phonons. Since these pioneering experiments more sophisticated methods of phonon generation have become available. These involve luminescent centres [2, 3], superconducting junctions [4], and stimulated emission [5, 6]. Far-infrared laser sources have been used to generate extremely monochromatic acoustic phonons [5, 7], and picosecond laser techniques have been applied to release coherent strains in crystals [8]. Conventional heaters are now widely used to generate phonons up to frequencies that typically are an order of magnitude smaller than zone-boundary frequencies [9]. In recent years, however, point contacts have proved to be suitable generators of high-frequency phonons [10]. Of the various realisations of point contacts, the contact used for the injection of phonons is of the spear-anvil type, i.e., a metal whisker pressed onto a metal film deposited on the crystal. As a phonon source, its dimensions are of the order of the thickness of the film.

The aim of this paper is to measure the frequency distribution of the injected phonons in terms of an effective temperature, and thus to evaluate the point contact as a generator of high-frequency phonons. Tungsten–tungsten contacts are chosen for the high melting point. The phonons are injected into a single crystal of dilute ruby (Al_2O_3:Cr^{3+}), first, because its lattice supports phonons up to high frequencies, and, second, because it permits Cr^{3+} maintained in the optically excited $\bar{E}(^2E)$ state to serve as a luminescent detector of these phonons. As it turn out, the ballistic regime beyond the 'hot spot' commences only a few micrometers below the point contact. For this reason, sufficient

0953-8984/90/326721 + 09 $03.50

spatial resolution cannot be achieved by the standard luminescent detection, which relies on a focused laser beam exciting the Cr^{3+}. In the present paper, advantage is taken of the shift of the R_1 line towards lower energy with increasing temperature [11]. Substantial gradients in the phonon occupation are present near the hot spot. So shells about the point contact of various 'temperatures' are selected *within* the laser beam via their specific shift of the R_1 transition. A non-equilibrium phonon distribution further affects the homogeneous width of R_1 [12]. In the method worked out below, the measured shifts and homogeneous widths of the R_1 transition are combined to extract the phonon distribution pertaining to various depths.

2. Experimental details

The specimen is a 700 at.ppm ruby single-crystal, $15 \times 10 \times 7\ mm^3$ in size. The point contacts were made of an electrochemically etched W whisker pressed onto a 500-Å W film sputtered onto the crystal in a Kr atmosphere. The resistance of the contact typically was 50 Ω at room temperature. Voltages of up to 16 V were applied. The reflection of superimposed negative pulses was used to monitor the impedance of the contact *in situ*. The power dissipated amounted to a maximum of 2 W. To remove thermal phonons, the crystal was kept at 1.5 K by immersion in pumped liquid helium. The Cr^{3+} ions necessary for the measurement of the effective phonon temperature via the R_1 luminescence (693 nm) were excited directly to the $\bar{E}(^2E)$ state by means of an actively stabilised single-frequency dye laser (bandwidth $\leq$1 MHz) pumped with an argon ion laser. In order that the laser beam (diameter ~90 μm) could be as close to the point contact as possible, the geometry chosen was such that the laser beam ran through the crystal and was reflected off the film at an angle of 10°. To ensure precise overlap of the laser beam and the hot spot, the beam was positioned so as to achieve maximum R_2 intensity when the laser frequency was set at the centre of the R_1 line. The R_2 intensity is used here as a gauge for the occupation of 29 cm^{-1} phonons resonant with the $\bar{E}(^2E) - 2\bar{A}(^2E)$ excited-state transition of Cr^{3+} [2, 13]. The outgoing R_1 light was detected with conventional photon-counting techniques after passing through a 0.85 m double monochromator to suppress any undesired luminescence.

As already noted, the detection volume is selected by tuning the laser away from the position of the R_1 line at 1.5 K towards longer wavelengths. Of course, this works best very near the point contact where the effective temperature exhibits the steepest gradient. The maximum observed shifts of the R_1 line amounted to 40 GHz, which is substantially larger than the inhomogeneous linewidth of 3.6 GHz. Larger shifts would be attainable, were it not for the drastic reduction in the detected volume and the severe line broadening with increasing temperature. At a distance of 90 μm from the film, at the opposite side of the reflecting laser beam, the shift has dropped to less than the linewidth. The laser frequency was calibrated with reference to the 1.5 K R_1 resonance using an optical spectrum analyser (free spectral range = 2 GHz, finesse > 200).

The homogeneous width of the R_1 line, the second ingredient needed for the determination of the effective temperature, was measured with the technique of fluorescence line narrowing (FLN). With this technique, the inhomogeneity of the optical transition is eliminated by restricting the excitation of Cr^{3+} to a single homogeneous packet. Under these conditions, the spectral width of the emitted fluorescence equals twice the homogeneous width of the R_1 transition. The determination of this width with FLN requires narrow-band excitation in conjunction with high-resolution optical detection.

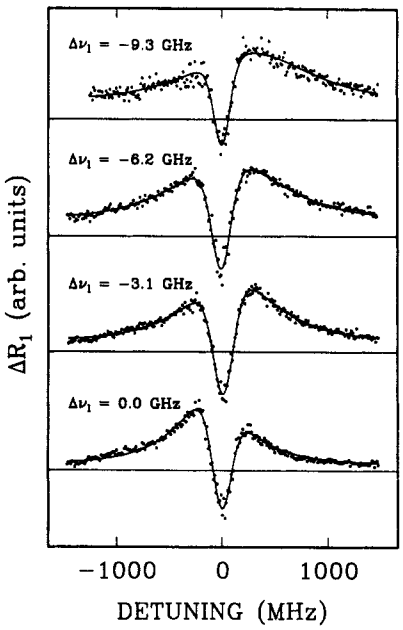

Figure 1. Typical FLN spectra at various settings of the laser frequency with respect to the resonance frequency at 1.5 K.

To this end, a single-pass temperature-stabilised scanning Fabry–Perot interferometer (free spectral range = 3.5 GHz, finesse > 30) was placed in front of the monochromator.

In addition to the signal related to phonons injected by the point contact, the spectra contain contributions from disturbed Cr^{3+} which have their line positions displaced towards lower energies by, for instance, being part of exchange-coupled pairs [14]. To remove the associated undesired signal, which in most cases exceeds the FLN signal of the temperature-shifted ions, scans through the R_1 spectrum are registered alternately in the presence and in the absence of heat pulses. The difference signal was subsequently accumulated to improve the statistics. Another complication is that the heat pulses lead to an increased pumping into $\bar{E}(^2E)$. This is a direct consequence of the associated redistribution over the populations within the $^4A_2$ ground state, which is split into $M_J = \pm\frac{1}{2}$ and $\pm\frac{3}{2}$ substrates separated by 11.4 GHz. The effect was eliminated by modulating the laser beam at a rate faster than the redistribution with $^4A_2$ (1 ms on, 1 ms off), by blocking the detector during the laser-off period, and by synchronously gating the pulse generator supplying the heat pulses in such a way that the heat pulses were injected during the laser-on period in the signal add mode and during the laser-off period in the subtract mode.

3. Results and discussion

In figure 1 we present typical differential FLN spectra of the temperature-shifted R_1 luminescence with the laser set exactly at the centre of the 1.5 K R_1 resonance frequency ($\Delta\nu_l = 0$), and with the laser frequency shifted by $\Delta\nu_l = -3.1$, -6.2, and -9.3 GHz. The spectra appeared not to be affected by the laser power. The spectrum with the laser set at the centre of R_1 ($\Delta\nu_l = 0$) contains contributions from Cr^{3+} ions whose R_1 transitions are shifted by, on the average, less than half the inhomogeneous width

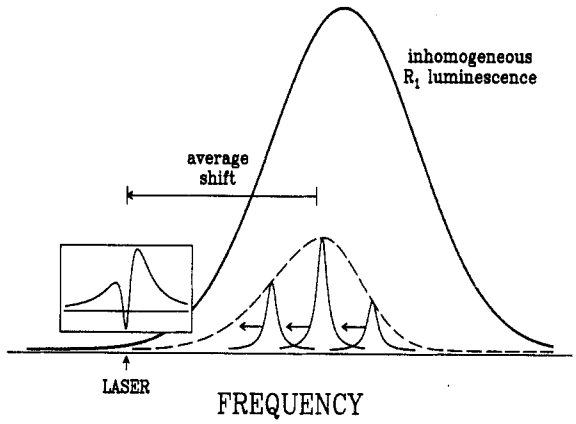

Figure 2. Phonon-induced shifts experienced by homogeneous R_1 packets. All shifts are to lower frequencies, and are accompanied by additional homogeneous broadening. Fractions of these packets, as indicated schematically by the dashed line, are displaced to coincide with the laser. In turn, the packet resonant with the laser in the absence of phonons is partly shifted away, causing the dip. The resultant spectrum is shown in the inset.

($\simeq$1.8 GHz). The other spectra in figure 1 have been selected by tuning the laser to frequencies below the low-temperature R_1 line. These spectra thus originate from Cr^{3+} ions located nearer the point contact. The homogeneous width of the R_1 transition apparently becomes larger and its intensity weaker as the frequency shift increases.

At this point, it is important to comprehend precisely what has been recorded. Positive contributions to the spectra originate from those parts of the various homogeneous packets of the inhomogeneously broadened R_1 line that are shifted so that they coincide with the laser frequency (figure 2). Note that the only shifts that occur are towards *lower* frequency. For $|\Delta\nu_l|$ up to, say, 3.6 GHz, these contributions thus stem from relatively 'cold' Cr^{3+} whose transitions are only minutely shifted, and further from 'warmer' homogeneous packets that have come from the other side of the R_1 line. The negative contribution to the spectra consists of those parts of the resonant homogeneous packets of the 'cold' R_1 line that have shifted out of resonance by the phonons. In the semi-spherical symmetry of the point contact, the R_1 intensity preferentially stems from further shells where the shifts are smaller. In figure 2 this is indicated by the asymmetry of the dashed curve. The geometrical emphasis on smaller shifts leads to the kind of asymmetry observed in the spectra. Note that the asymmetry is, as it should be, reversed for the $\Delta\nu_l = 0$ spectrum.

From spectra such as those in figure 1 the homogeneous width has been extracted by means of the following procedure: (i) the positive contributions are assumed to add up to a Lorentzian; (ii) the negative contributions, which are known to have a Voigt profile by virtue of residual inhomogeneous broadening [15], are adequately approximated by a Lorentzian to a power near unity; (iii) the result is convoluted with the interferometer transmission profile derived from a separate experiment; (iv) account is taken of neighbouring orders of the interferometer transmission; and (v) the widths and positions of the two Lorentzians are least-squares adjusted to the data, while repeating steps (iii) and (iv) until self-consistency is obtained. Note that in an FLN experiment the width of a Lorentzian equals twice the width of the corresponding homogeneous line. The fits are represented by the solid curves in figure 1. The results for the homogeneous width of the R_1 line, $\Delta\nu_{hom}$, associated with a shift δE, are collected in table 1.

Table 1. Shifts and homogeneous widths of the R_1 line measured with FLN at various settings of the laser frequency, and derived temperatures T_0 and distances R in units R_0.

$\Delta\nu_l$ (GHz)	δE (GHz)	$\Delta\nu_{hom}$ (GHz)	T_0 (K)	R/R_0
0	-1.8 ± 0.5[a]	0.39 ± 0.02	415 ± 50	24 ± 5
−3.1	-3.1 ± 0.5	0.53 ± 0.02	380 ± 40	17 ± 3
−6.2	-6.2 ± 0.5	0.69 ± 0.02	320 ± 20	10.3 ± 0.7
−9.3	-9.3 ± 0.5	0.88 ± 0.02	285 ± 15	7.4 ± 0.5

[a] Shift estimated to be half the inhomogeneous line width on the grounds that for $\Delta\nu_l = 0$ only the high-frequency half of R_1 transition is relevant.

When performing an analysis in terms of local phonon densities, one should realise that, irrespective of the precise form of their spectrum, the injected phonons at first undergo a diffusive motion leading to thermalisation. At temperatures of several hundreds of kelvin, the scattering is brought about by phonon–phonon processes. Classical heat-conductivity data indicate that the phonon mean free path, Λ, then is minute in relation to the micrometre scale of the experiment. In Al_2O_3 at 300 K, as a case in point, the heat-conductivity coefficient κ amounts to 0.5 W cm^{-1} K^{-1} [16], from which by use of $\kappa = \frac{1}{3}C_V\Lambda v$ it follows that $\Lambda \sim 0.05\,\mu$m. Here, $C_V \simeq 3Nk_B$ is the heat capacity, $v \simeq 7$ km s^{-1} is the velocity of sound averaged over the modes, and N the number of unit cells per cm^3. After a few micrometres, therefore, sufficient collisions have occurred to ensure thermalisation, except perhaps at the lowest frequencies ($\lesssim$2 THz). Beyond this point the phonons may continue to travel diffusively, resulting in a spread of the energy over a large shell with a corresponding decrease of the effective temperature of the distribution. Soon, however, the energy is diluted to such an extent that Λ is comparable to the dimensions of the excited zone, i.e., the phonons escape ballistically. The escape, of course, occurs earlier for phonons of lower energy. The transport of 1 THz phonons through Al_2O_3 kept at low temperatures has been examined directly in time-of-flight experiments [14]. Mean free paths of at least 1 cm were found, corresponding to lifetimes exceeding several μs. At low energy densities the prevailing decay process is anharmonic break up, whose rate initially scales with the fifth power of the frequency, but increases somewhat slower at higher frequencies because of the increasing failure to conserve both energy and momentum. For phonons of, say, 5 THz, extrapolation yields Λ's against spontaneous decay of the order of tens of μm at low phonon densities.

In relating the measured widths and shifts of the R_1 luminescence to local phonon densities, one first notes that, except at very low phonon densities, the dephasing of the $\bar{E}(^2E)$ level is determined by phonon processes connecting $\bar{E}(^2E)$ and $2\bar{A}(^2E)$ [11]. In the first instance, direct processes between $\bar{E}(^2E)$ and $2\bar{A}(^2E)$ are responsible for the phonon-induced part of the homogeneous width. When the temperature is raised further, however, Raman processes between $\bar{E}(^2E)$ and $2\bar{A}(^2E)$ soon dominate the width of $\bar{E}(^2E)$. These contributions can be calculated by the use of perturbation theory up to second order. In the Debye approximation of the density of states, the homogeneous width quite generally equals

$$\Delta\nu_{hom} = \Delta\nu_0 + \frac{\pi\beta}{\nu_D^3}\Delta^3 n(\Delta) + \frac{\alpha}{\nu_D^7}\int_0^{\nu_D} \nu^6 n(\nu)[n(\nu)+1]\,d\nu \qquad (1)$$

where $n(\nu)$ is the phonon occupation at frequency ν, Δ is the $\bar{E}(^2E) - 2\bar{A}(^2E)$ resonance

frequency, α and β contains the matrix elements for Raman and direct processes, respectively, ν_D is the Debye cut-off frequency, and $\Delta\nu_0$ is the residual width at low temperatures ($\lesssim$10 K). The latter is determined by the hyperfine interactions between the Cr^{3+} electron spin and the surrounding Al nuclear spins, whose fluctuating magnetic field at the Cr^{3+} site modulates the R_1 resonance frequency via a dynamic Zeeman effect. From previous FLN and hole-burning experiments [15], this width is known to amount to 65 MHz in zero magnetic field.

A finite phonon density further modifies the position of the energy levels of the Cr^{3+} ions, and as a result the R_1 line shifts towards lower frequencies. In a good approximation, this shift scales with the energy stored in the lattice [17]. Within the Debye approximation, and with account of the nearby $2\bar{A}(^2E)$ level at a distance Δ, we have for the R_1 line shift

$$\delta E = \frac{\beta\Delta}{\nu_D^3}\mathcal{P}\int_0^{\nu_D}\frac{\nu^3 n(\nu)}{\nu^2-\Delta^2}\,d\nu + \frac{\alpha'}{\nu_D^4}\int_0^{\nu_D}\nu^3 n(\nu)\,d\nu \tag{2}$$

where $\mathcal{P}$ denotes taking the principal value of the integral. If an effective temperature T is a meaningful quantity, (1) and (2) reduce to the more common forms [11, 18]

$$\Delta\nu_{hom}(T) = \Delta\nu_0 + \pi\beta\left(\frac{T_\Delta}{T_D}\right)^3 n(\Delta) + \alpha\left(\frac{T}{T_D}\right)^7\int_0^{T_D/T} x^6 n(x)[n(x)+1]\,dx \tag{3}$$

$$\delta E(T) = \beta\frac{T_\Delta}{T_D}\left(\frac{T}{T_D}\right)^2\mathcal{P}\int_0^{T_D/T} x^3 n(x)\frac{1}{x^2-(T_\Delta/T)^2}\,dx + \alpha'\left(\frac{T}{T_D}\right)^4\int_0^{T_D/T} x^3 n(x)\,dx \tag{4}$$

where $x = h\nu/k_BT$, $T_D = h\nu_D/k_B$ and $T_\Delta = h\Delta/k_B$. For thermal phonons, $n(x) = (e^x-1)^{-1}$. As far as the relative weights of the α and β terms are concerned, calculations in connection with the analysis below show that in both $\Delta\nu(T)$ and $\delta E(T)$ the β part grows much more slowly with T. For thermal phonon populations, the α and β terms in $\Delta\nu_{hom}(T)$ balance at approximately 60 K, whereas in $\delta E(T)$ the α part already predominates at temperatures as low as 20 K. The β terms are only about 2% of their α counterparts at 150 K, and less than 1% at 300 K.

For a calibration of the width and position of the R_1 line as probes to measure phonon densities, we briefly consider the effects of a thermal phonon occupation. For this case, McCumber and Sturge [11] determined the part associated with the Raman processes, which predominates in the high-temperature regime. By analysing the temperature-dependent width of the inhomogeneous R_1 line above 90 K on the basis of (3), they found $\alpha = 544\ cm^{-1}$ and $T_D = 760$ K. The high-temperature data do not allow a determination of β. The contribution of the direct process can, however, be discerned if the inhomogeneous broadening of the optical transition is eliminated by the use of FLN. In figure 3, we present the width of the R_1 line as measured with FLN at temperatures sufficiently low for Raman processes to be at least one order of magnitude smaller. In this experiment the free spectral range of the interferometer was reduced to 2.5 GHz. The solid curve in figure 3 represents a least-squares fit of (3) to the data points with the α part being ignored. The fit yielded $\pi\beta(T_\Delta/T_D)^3 = 235 \pm 20$ MHz, resulting in $\beta = 14.45 \pm 1.2\ cm^{-1}$. The fitted result for $\pi\beta(T_\Delta/T_D)^3$ is directly identifiable with the homogeneous width of $2\bar{A}(^2E)$. We thus find $\Delta\nu_{2\bar{A}} = 235 \pm 20$ MHz, which is in excellent agreement with estimates from other frequency-selective [19, 20] and time-resolved [21]

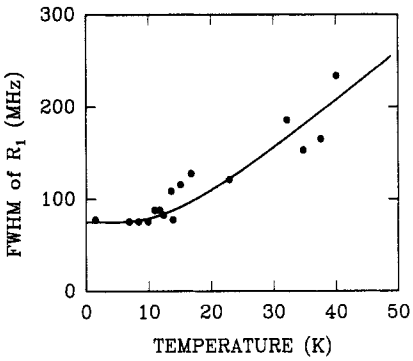

Figure 3. Temperature dependence of the homogeneous width of the R_1 transition.

experiments. From the data on the line shift $\delta E(T)$ at temperatures extending to 700 K, McCumber and Sturge [11] further found $\alpha' = -400\,\mathrm{cm}^{-1}$ by use of (4), again with neglect of the β part. Although their analysis was based on the Debye approximation, (3) and (4) appear to describe the experiments accurately up to a substantial fraction of T_D. This provides considerable justification for using (3) and (4) to determine the temperature of the injected phonons from the R_1 luminescence.

In carrying out the actual analysis, we used the fact that the moment the phonons become ballistic their energy distribution does not appreciably alter except for an overall reduction with distance. In other words, the phonon spectrum remains essentially of the *shape* of the Planckian distribution adopted at the outer boundary of the diffusive regime. This, in effect, also makes the point contact suitable as a generator of high-frequency phonons. The assumptions underlying the model worked out below accordingly are as follows: (i) The phonons initially travel diffusively while breaking up and recombining by anharmonic processes to achieve a Planckian distribution of their energies on the surface of a hemisphere with radius R_0 about the point contact; (ii) this hemisphere (hot spot) subsequently acts as an isotropic black-body radiator with effective temperature T_0; and (iii) beyond this hemisphere the motion of the phonons is entirely ballistic, i.e., the phonon occupations emitted by the radiator remain distributed according to the temperature T_0, but diminish with distance such that the total flux is conserved. (At the point of detection the mean free path of the last generation in the Levinson sense [22] is already much larger than the typical dimension of the detection zone. The spherical symmetry helps to dilute the phonon occupations with distance, thereby rapidly diminishing phonon–scattering.) The occupation number of phonons with frequency ν at distance R from the point contact may be derived by straightforward integration of the phonon flux at R over the surface of the black-body radiator. It then follows that along the direction perpendicular to the crystal surface ($R \geq R_0$)

$$n(\nu) = (R_0^2/R^2)[\exp(h\nu/kT_0) - 1]^{-1}. \tag{5}$$

The phonon spectrum $n(\nu)$ is subsequently inserted into (1) and (2), and the resultant expressions are solved for the temperature T_0 and the ratio R/R_0, given the shift of R_1 and the associated homogeneous width (table 1). It is noted that the expressions are quadratic in R/R_0, but that the second solution for T_0 and R/R_0 is physically unrealistic ($R/R_0 < 1$ and δE increasing with R).

The results of the analysis are presented in table 1. The errors quoted for the resultant T_0 and R/R_0 are plain fitting errors, primarily due to the inhomogeneous broadening of the R_1 transition, which limits the precision with which δE can be determined. It should

be realised, however, that additional uncertainties result from the idealised form of equation (5) and the approximate allowance made for the variation of the phonon intensity over the luminescing region. These uncertainties do not, however, detract from the principal conclusion of this work that phonon temperatures of several hundreds of kelvin are reached in the point contact area. As anticipated, the larger shifts and widths stem from Cr^{3+} located nearer the point contact. It is inherent in the method that the distance can only be determined relative to the radius of the hot thermalisation volume. A rough estimate of R_0 may however be achieved from the present results. In the experiment the laser beam was focused down to approximately 90 μm, which, combined with the largest R/R_0 observed, places an upper limit of 4 μm on R_0. It should be pointed out, however, that ratios R/R_0 of over about 20 are associated with shifts already smaller than the inhomogeneous linewidth. Larger R/R_0, corresponding to smaller R_0 have therefore escaped measurement, even if the laser beam was sufficiently wide. An approximate lower limit for R_0 is the radius of the contact area of the point contact augmented with the film thickness, i.e., a few multiples of 0.1 μm. It is further noteworthy that the temperature T_0 is not strictly independent of the distance, as assumed in the model, but increases slightly with R. In other words, while the phonons travel away from the radiator, the occupations at the higher frequencies drop more slowly with distance than do the occupations at low frequencies. The latter occupations fall according to $1/R^2$ as is appropriate for ballistic transport. The most likely cause is residual elastic scattering by imperfections like Cr^{3+} ions, which is proportional to ν^4.

4. Conclusions

The principal results of this paper are the following: (i) A metal–metal point contact acts as a point source of non-equilibrium phonons up to high frequencies, and (ii) a detector of phonons based on FLN can be successfully used to investigate the phonon occupations selectively in space via phonon-induced shifts of the R_1 luminescence in combination with the associated homogeneous broadening. Close to the point contact, where phonon temperatures as high as 300 K are reached and the gradients are substantial, the detector measures up to the generator as far as spatial resolution is concerned. The combination thus permits the examination of high-frequency phonons with their intrinsic short mean free path. The method has been employed here is a quasi-stationary way, but could be extended to the time domain by applying transient excitation and detection of the development of the spectral shifts with time. Finally, it is noted that another detector that could be usefully combined with a point contact is the standard luminescent ruby detector, which relies on the R_2 luminescence as a measure of the phonon occupation. The detector is preferentially sensitive to 29 cm^{-1} phonons. If, however, it were combined with narrow-band excitation directly into the low-energy wing of $\bar{E}(^2E)$, it should be possible to achieve comparable spatial resolution.

Acknowledgments

The authors thank C R de Kok for invaluable technical assistance. The work was financially supported by the Netherlands Foundation 'Fundamenteel Onderzoek der Materie' and the 'Nederlandse Organisatie voor Wetenschappelijk Onderzoek'.

References

[1] von Gutfeld R J and Nethercot A H 1964 *Phys. Rev. Lett.* **12** 641
[2] Dijkhuis J I, van der Pol A and de Wijn H W 1976 *Phys. Rev. Lett.* **37** 1554

[3] Meltzer R S and Rives J E 1977 *Phys. Rev. Lett.* **38** 421
[4] Berberich P, Burmann R and Kinder H 1982 *Phys. Rev. Lett.* **49** 1500
Berberich P and Kinder H 1983 *Phonon Scattering in Condensed Matter* ed W Eisenmenger, K Lassmann and S Döttinger (Heidelberg: Springer) p 18
[5] Bron W E and Grill W 1978 *Phys. Rev. Lett.* **40** 1459
[6] Hu P 1980 *Phys. Rev. Lett.* **44** 417
[7] Lengfellner H and Renk K F 1977 *IEEE J. Quantum Electron.* **QE-13** 421
[8] Thomson C, Strait J, Vardeny Z, Maris H J and Tauc J 1984 *Phys. Rev. Lett.* **53** 989
[9] Bron W E 1980 *Rep. Prog. Phys.* **43** 301
[10] Goossens R J G, Dijkhuis J I and de Wijn H W 1985 *J. Lumin.* **34** 19
[11] McCumber D E and Sturge M D 1982 *J. Appl. Phys.* **34** 1682
[12] Meltzer R S and Macfarlane R M 1985 *Phys. Rev.* B **28** 4786
[13] Renk K F and Deisenhofer J 1971 *Phys. Rev. Lett.* **26** 764
[14] Basun S A, Kaplyanskii A A and Feofilov S P 1986 *Fiz. Tverd. Tela* **28** 3616 (Engl. Transl. 1986 *Sov. Phys.–Solid State* **28** 2038)
[15] Jessop P E, Muramoto T and Szabo A 1980 *Phys. Rev.* B **21** 926
[16] 1970 *Thermal Physical Properties of Matter (Thermal Conductivity-Nonmetallic Solids 2)*, ed Y S Touloukian, R W Powell, C Y Ho and P G Klemens (New York: Plenum)
[17] Imbusch G F, Yen W M, Schawlow A L, McCumber D E and Sturge M D 1964 *Phys. Rev.* **133** A1029
[18] Di Bartolo B 1968 *Optical Interactions in Solids* (New York: Wiley) p 367
[19] Retzer N, Lengfellner H and Renk K F 1983 *Phys. Lett.* **96A** 487
[20] van Dort M J, Dijkhuis J I and de Wijn H W 1989 *Solid State Commun.* **72** 237
[21] Rives J E and Meltzer R S 1977 *Phys. Rev.* B **16** 1808
Overwijk M H F, de Kok C R, Dijkhuis J I and de Wijn H W 1990 *J. Lumin.* **45** 449
[22] Levinson Y B 1986 *Nonequilibrium Phonons in Nonmetallic Crystals* ed W Eisenmenger and A A Kaplyanskii (Amsterdam: North-Holland)